Molecular basis of binding between MERS-CoV and CD26s from 7 bat species

Supporting Information includes

Tables S1

Figures S1-S3

References for SI reference citations

Table S1. Comparison of MERS-RBD binding to MD bCD26 and hCD26

Residues in MD bCD26/hCD26	MD bCD26/MERS-RBD	hCD26/MERS-RBD
—/T188	—	E536 (1)
N227/N229	NAG: W535 (4), E536 (16), NAG: W535 (22), D539 (2) BMA: W535 (5)	NAG: W535 (3), E536 (13), D539 (1) NAG: W535 (23), D539 (2) BMA: W535 (6)
—/T265	—	Y540 (3)
—/V266	—	Y540 (1)
K265/K267	D537 (3), G538 (5), D539 (2)	E536 (3), D537 (5), G538 (12), D539 (7)
Y267/F269	D537 (6)	D537 (5)
E278/T283	V561 (1)	—
Q281/Q286	N501 (2), G538 (4), S557 (2), G558 (1), S559 (1)	N501 (4), D537 (1), G538 (11), S557 (3), G558 (1), S559 (1)
V283/T288	N501 (1), K502 (3), S557 (6)	N501 (4), K502 (10), S557 (4)
A284/A289	K502 (4)	K502 (5)
P285/P290	K502 (4), E513 (3)	K502 (3), E513 (3)
A286/A291	K502 (3), S504 (2), L506 (1), E513 (10), V555 (6)	K502 (2), S504 (1), L506 (4), E513 (11), V555 (4)
S287/S292	L506 (9), D510 (2), R511 (1)	L506 (7), D510 (1)
L289/L294	Y540 (11),Y541 (1),R542 (4), V555 (6)	K502 (2), Y540 (7), R542 (8), V555 (4)
T290/I295	L506 (1), R542 (15), W553 (27), V555 (1)	L506 (3), D510 (3), R542 (12), W553 (28), V555 (2)
G291/G296	Y540 (9), R542 (9)	R542 (7)
D292/D297	Y540 (3)	R542 (1)
H293/H298	Y540 (7)	Y540 (7)
R312/R317	L506 (1), D510 (10)	L506 (1), D510 (11)
Y317/Y322	D510 (10), R511 (4)	D510 (4), R511 (4)
T329/S334	S460 (1),	S454 (1), D455 (1)
K331/R336	A461 (3), P463 (1), Q466 (2)	M452 (1), D455 (8), P463 (9), Y499 (10)
V336/V341	E513 (11), P515 (1)	E513 (9), P515 (2)
Q339/Q344	R511 (1), E513 (5)	E513 (5)
I341/I346	R511 (7)	R511 (11)
—/K392	—	R511 (2)
Total contacts	282	328

The number in the parentheses represent the number of van der Walls contacts, which the indicated residues conferred. The number in red suggest the potential H-bond between the pair of residues. In this table, van der Walls contact was analyzed at the cutoff of 4.5 Å and the H-bonds at the cutoff of 3.3 Å.

Supplemental figures and figure legends

		Pteropodidae				Rhinolophidae		Hipposideridae	Emballonuridae	Phyllostomidae				Miniopteridae	Vespertilionidae				
	H. sapien	***R. aegyptiacus***	***E. buettikoferi***	***P. vampyrus***	***P. alecto***	***R. ferrumequinum***	***R. sinicus***	***H. armiger***	***S. bilineata***	***A. planirostris***	***A. jamaicensis***	***C. perspicillata***	***D. rotundus***	***M. natalensis***	***E. fuscus***	***P. pipistrellus***	***M. lucifugus***	***M. davidii***	***M. brandtii***
H. sapien	100/ 100	88.73/ 83.94	88.60/ 82.48	88.20/ 81.75	88.85/ 82.48	86.09/ 81.75	86.50/ 81.75	84.89/ 81.62	85.56/ 82.48	84.51/ 81.75	84.38/ 81.02	83.99/ 81.75	84.78/ 83.21	83.99/ 81.75	84.74/ 83.70	82.37/ 78.83	83.60/ 80.29	82.52/ 76.64	83.71/ 80.29
R. aegyptiacus		100/ 100	96.46/ 94.16	94.63/ 92.70	94.88/ 91.24	87.40/ 84.67	88.73/ 86.13	87.91/ 84.56	86.86/ 81.02	85.70/ 80.29	85.83/ 81.02	84.78/ 79.56	85.56/ 79.56	84.91/ 81.02	86.18/ 82.22	83.03/ 77.37	84.78/ 78.10	83.57/ 75.91	84.63/ 79.56
E. buettikoferi			100/ 100	95.67/ 94.16	95.67/ 91.97	88.19/ 84.67	88.86/ 85.40	87.39/ 82.35	87.52/ 81.02	85.30/ 79.56	85.43/ 80.29	84.91/ 79.56	85.83/ 79.56	85.17/ 81.75	86.58/ 82.96	83.55/ 78.10	85.30/ 78.83	84.23/ 76.64	85.02/ 78.83
P. vampyrus				100/ 100	98.03/ 97.81	86.88/ 83.21	88.47/ 84.67	87.12/ 82.35	87.25/ 79.56	85.56/ 78.10	85.70/ 78.83	85.17/ 79.56	86.35/ 79.56	85.17/ 79.56	86.05/ 80.74	83.68/ 78.10	85.04/ 76.64	84.63/ 77.37	85.28/ 78.10
P. alecto					100/ 100	86.99/ 81.75	88.58/ 83.21	87.65/ 81.62	87.50/ 79.56	86.20/ 78.83	86.33/ 79.56	85.28/ 78.83	86.73/ 78.83	85.55/ 78.83	86.56/ 80.00	84.19/ 77.37	85.41/ 75.91	84.74/ 76.64	85.39/ 77.37
R. ferrumequinum						100/ 100	95.01/ 90.51	90.00/ 88.24	86.97/ 83.21	85.41/ 81.02	85.28/ 80.29	85.41/ 82.48	85.55/ 82.48	86.73/ 83.94	85.51/ 86.67	83.40/ 81.02	84.89/ 82.48	83.95/ 80.29	84.74/ 83.21
R. sinicus							100/ 100	91.72/ 88.24	87.25/ 80.29	85.70/ 80.29	85.56/ 79.56	85.83/ 81.02	86.22/ 81.02	87.01/ 81.02	86.05/ 82.96	84.61/ 82.48	85.04/ 80.29	84.36/ 78.10	85.02/ 81.02
H. armiger								100/ 100	85.38/ 80.88	84.47/ 80.88	84.34/ 80.15	84.87/ 83.09	85.13/ 83.09	85.79/ 80.88	84.85/ 82.22	82.98/ 80.88	85.00/ 82.35	83.79/ 79.41	84.85/ 83.09
S. bilineata									100/ 100	85.28/ 79.56	85.15/ 78.83	84.76/ 81.75	85.68/ 81.75	85.13/ 79.56	85.22/ 81.48	83.25/ 78.10	84.08/ 81.02	82.61/ 76.64	83.79/ 80.29
A. planirostris										100/ 100	99.87/ 99.27	94.12/ 89.78	93.20/ 89.78	84.91/ 81.75	84.21/ 80.74	83.42/ 76.64	83.86/ 78.83	82.39/ 74.45	83.97/ 78.83
A. jamaicensis											100/ 100	93.99/ 89.05	93.07/ 89.05	85.04/ 82.48	84.08/ 80.00	83.29/ 75.91	83.73/ 78.10	82.26/ 73.72	83.84/ 78.10
C. perspicillata												100/ 100	94.12/ 94.16	84.91/ 83.21	84.61/ 82.22	83.95/ 82.48	84.78/ 83.21	83.71/ 80.29	84.76/ 83.21
D. rotundus													100/ 100	86.22/ 82.48	85.79/ 83.70	84.34/ 81.02	84.51/ 81.75	83.44/ 78.83	84.63/ 81.75
M. natalensis														100/ 100	88.68/ 85.93	85.66/ 80.29	87.27/ 83.21	85.94/ 81.75	86.86/ 83.94
E. fuscus															100/ 100	93.80/ 88.89	93.68/ 91.85	92.62/ 88.15	93.41/ 91.85
P. pipistrellus																100/ 100	90.79/ 86.86	90.25/ 86.13	90.65/ 87.59
M. lucifugus																	100/ 100	96.58/ 93.43	97.63/ 97.08
M. davidii																		100/ 100	96.97/ 94.16
M. brandtii																			100/ 100

Figure S1. Diversity of bCD26s and homologies to hCD26. The percent identity matrix among bCD26s and hCD26 is displayed. In each pair of comparisons, the former number indicates the percent identity of the full-length CD26, and the latter number represents the percent identity of the region spanning blades IV and V. The family name of each species of bat is marked above the matrix and in the same color as the name of the species.

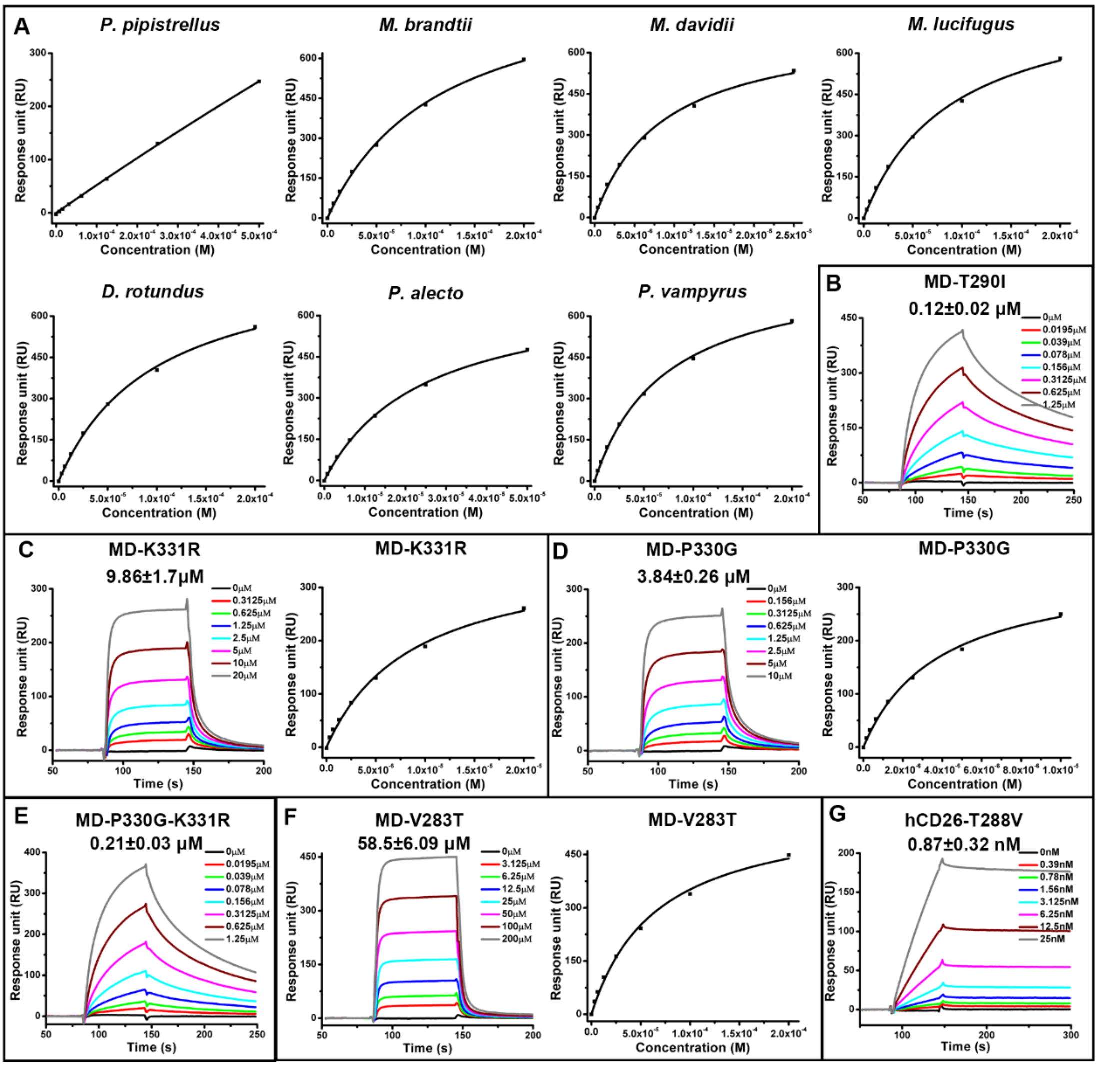

Figure S2. The interactions between MERS-RBD and the indicated CD26s. (A) The saturation profiles for the indicated binding pairs characterized in the SPR assay, which are related to Figure 1. (B-F) The interaction between MERS-RBD and MD CD26 and hCD26-T288V mutations. The upper panel indicates the binding profile, and the lower panel represents the saturation curves. (B) MD-T290I binding to MERS-RBD. (C) MD-K331R binding to MERS-RBD. (D) MD-P330G binding to MERS-RBD. (E) MD-P330G-K331R binding to MERS-RBD. (F) MD-V283T binding to MERS-RBD. (G) hCD26-T288V binding to MERS-RBD.

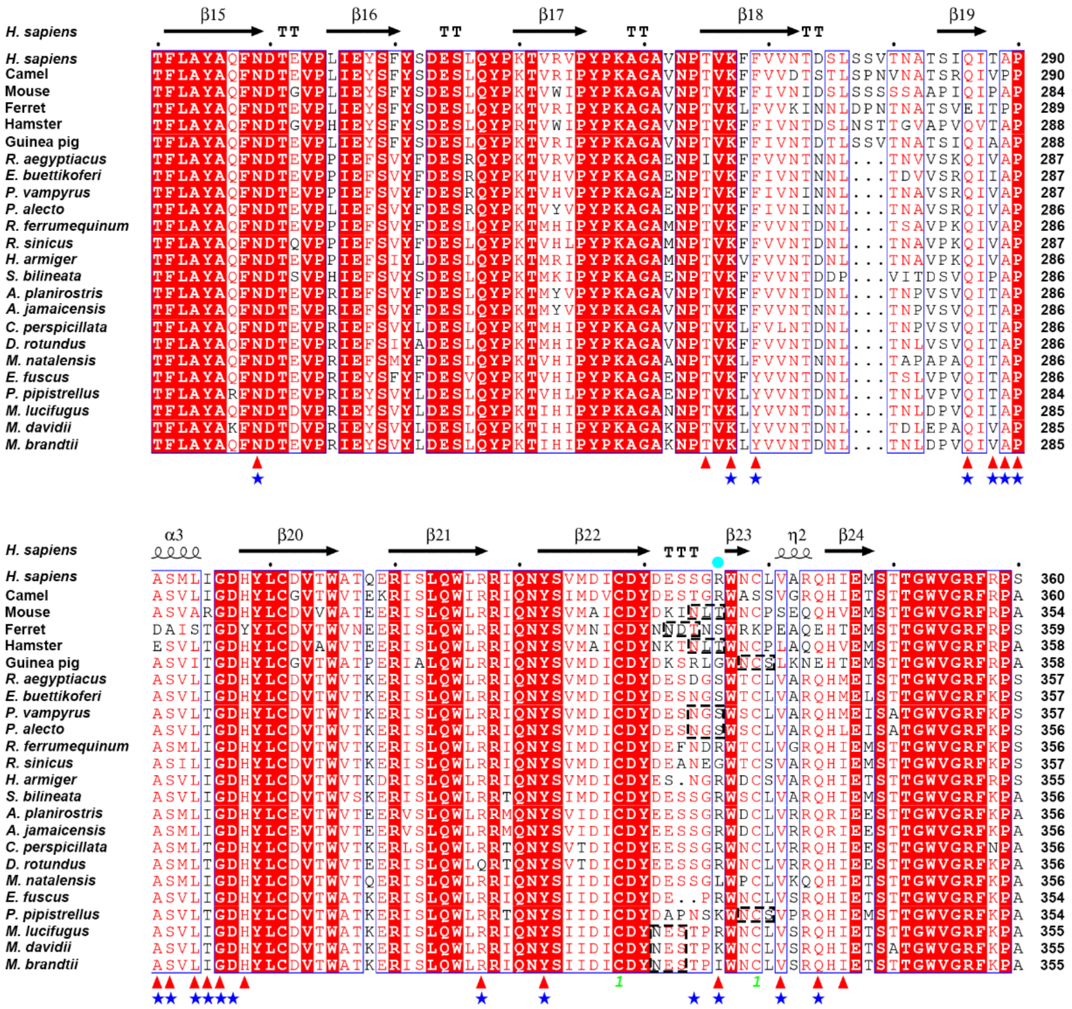

Figure S3. Structure-based sequence alignment. The secondary structure elements are defined based on an ESPript (1) algorithm and are labeled as in a previous report on the MERS-RBD structure (2). Spiral lines indicate α or 3_{10} helices, while arrows represent β strands. The Arabic numeral 1 indicates cysteine residues that pair to form disulfide bonds. The residues located within the distance of 4.0 Å in the interaction interface were analyzed and marked. The ones in hCD26 that bind MERS-RBD are highlighted with red triangles, and the MD bCD26 residues that bind MERS-RBD are indicated with blue stars. The cyan circle above the sequences indicates R336 in hCD26. Glycosylation motif around hCD26 R336 equivalents among species and bats are highlighted with dashed boxes.

References for SI reference citations

1. Gouet P, Courcelle E, Stuart DI, Metoz F. 1999. ESPript: analysis of multiple sequence alignments in PostScript. Bioinformatics 15:305-308.
2. Lu G, Hu Y, Wang Q, Qi J, Gao F, Li Y, Zhang Y, Zhang W, Yuan Y, Bao J, Zhang B, Shi Y, Yan J, Gao GF. 2013. Molecular basis of binding between novel human coronavirus MERS-CoV and its receptor CD26. Nature 500:227-31.